

A Low Complexity Quantum Principal Component Analysis Algorithm

CHEN HE^{1,2}, JIAZHEN LI¹, WEIQI LIU¹, Z. JANE WANG², Fellow, IEEE

¹Northwest University, Xi'an, China

²The University of British Columbia, Vancouver, BC, Canada

arXiv:2010.00831v2 [quant-ph] 13 Jan 2021

ABSTRACT In this paper, we propose a low complexity quantum principal component analysis (qPCA) algorithm. Similar to the state-of-the-art qPCA, it achieves dimension reduction by extracting principal components of the data matrix, rather than all components of the data matrix, to quantum registers, so that samples of measurement required can be reduced considerably. However, the major advantage of our qPCA over the state-of-the-art qPCA is that it requires much less quantum gates. In addition, it is more accurate due to the simplification of the quantum circuit. We implement the proposed qPCA on the IBM quantum computing platform, and the experimental results are consistent with our expectations.

INDEX TERMS Quantum Computing, Quantum Principal Component Analysis, Quantum Singular Value Threshold.

I. INTRODUCTION

Principal component analysis (PCA) [1]–[4] is widely employed in signal processing and machine learning for dimension reduction, and has a time complexity of $O(N^3)$, where N is the dimension of the data. When the dimension of the data is large, the classical PCA becomes non-tractable. Quantum principal component analysis algorithm (qPCA) can reduce the time complexity to $O(N \text{poly}(\log N))$ [5]–[7] because of the quantum computer's parallelism [8].

The qPCA in [5] outputs the quantum state containing all the eigenvalues and eigenvectors of the data, and the top- t components (principal components) are obtained by sampling. For instance, for a matrix $A_0 \in \mathbb{C}^{p \times q}$, let $A = \sum_{k=1}^r \lambda_k u_k u_k^T$ be the eigendecomposition of $A = A_0 A_0^+$, where A_0^+ is the conjugate transpose of A_0 . The qPCA in [5] showed that phase estimation can be employed to extract all eigenvalues λ_k and eigenvectors u_k into quantum registers with time complexity $O(r \text{poly}(\log p))$, i.e. the qPCA outputs the quantum state

$$|\psi_A\rangle = \sum_{k=1}^r \lambda_k |\lambda_k\rangle |u_k\rangle. \quad (1)$$

However, since $|\psi_A\rangle$ contains all the r components of A , the qPCA in [5] may need a lot of samples to obtain the principle components. To avoid this disadvantage, [9] proposed an improved qPCA as shown in Fig. 1, which yields a quantum state containing the approximation of the components with

the top t ($t \ll r$) largest eigenvalues only:

$$|\psi'_A\rangle \approx \sum_{k=1}^t \sigma_k |\lambda_k\rangle |u_k\rangle |v_k\rangle, \quad (2)$$

where σ_k are the singular values of A_0 , u_k, v_k are the left and right singular vectors respectively. As a result, the successful probability of obtaining a principal component increases to $\sum_{k=1}^r \lambda_k^2 / \sum_{k=1}^t \lambda_k^2$ times for each measurement, and the time complexity is also reduced to $O(t \text{poly}(\log p))$. The quantum circuit for obtaining $|\psi'_A\rangle$ by the qPCA [9] is shown in Fig. 1.

However, there are still two concerns for state-of-the-art qPCA in [9]. One is that the algorithm requires a lot of quantum gates, and the other is that the approximation is taken in two places, which may lead to a lower accuracy. In this paper, we propose a low complexity qPCA algorithm shown in Fig. 2. Compared with the state-of-the-art qPCA [9], the quantum circuit of our algorithm requires much less quantum gates, and the approximation is only taken in one place. The paper is organized as follows: In Section II, we proposed a low complexity qPCA algorithm. In Section III, we analyze the complexity and accuracy of our qPCA algorithm compared with state-of-the-art algorithm. In Section IV, we implement the proposed algorithm on IBM Quantum Experience, and verify the proposed algorithm. Finally we conclude this work in Section V.

II. THE PROPOSED QPCA

In this section, we introduce the procedures of our low complexity qPCA algorithm and design the corresponding

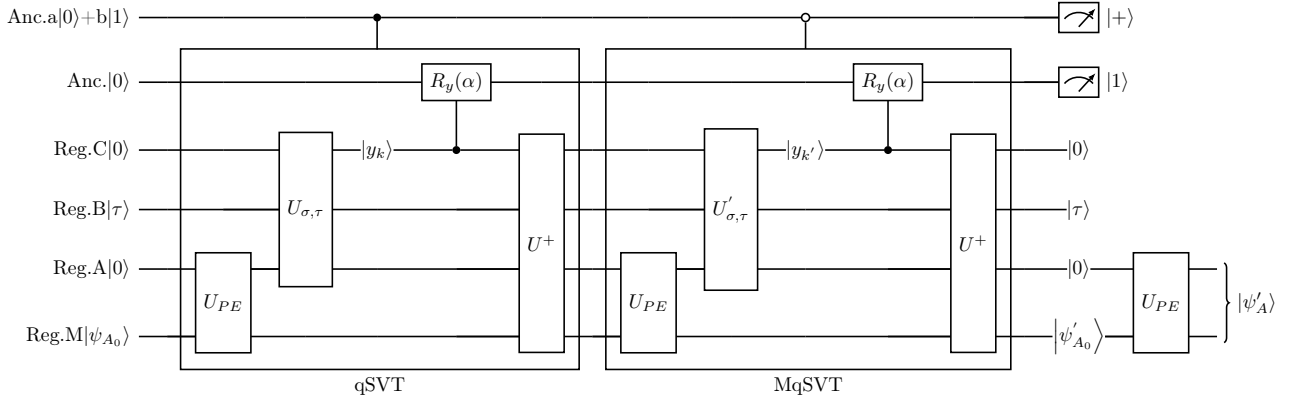


FIGURE 1: The quantum circuit of the qPCA proposed in [9], which consists of two parts: quantum singular values threshold (qSVT) [10] and modified qSVT (MqSVT). The input of the circuit is $|\psi_{A_0}\rangle$, and the output is $|\psi'_A\rangle$, where the principal components are in the quantum registers. In the circuit $y_k = (1 - \frac{\tau}{\sigma_k})_+$, $y'_k = (1 + \frac{\tau}{\sigma_k})_+$, τ is the threshold to filter out the small σ_k 's, and α is the parameter of rotation operation $R_y(\alpha)$, which can be adjusted to improve the success probability and fidelity of the algorithm.

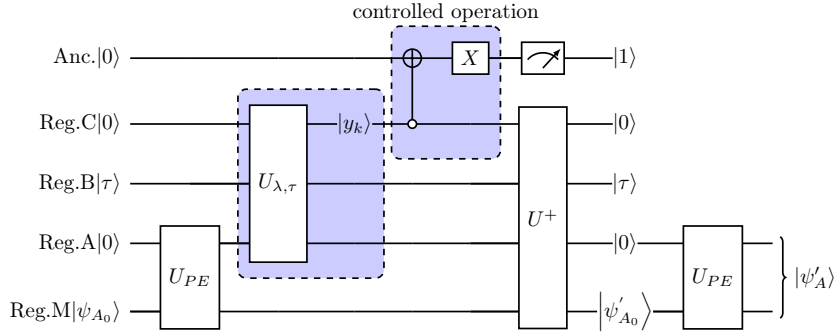


FIGURE 2: The quantum circuit of the proposed qPCA. The input of the circuit is $|\psi_{A_0}\rangle$ and the output is the quantum state $|\psi'_A\rangle$, where the principal components are in the quantum registers. In this circuit, $y_k = (1 - \frac{\tau}{\lambda_k})_+$, and τ is the threshold to filter out small λ_k 's. As we can see the quantum circuit of the proposed qPCA requires much less quantum gates compared with the state-of-arts in [9].

quantum circuit.

The quantum state of the matrix $A_0 = \sum_{k=1}^r \sigma_k u_k v_k^T$ is given by [10]

$$|\psi_{A_0}\rangle = \sum_{k=1}^r \sigma_k |u_k\rangle |v_k\rangle. \quad (3)$$

The purpose of qPCA is to extract the larger eigenvalues of the $A_0 A_0^+$ from the amplitudes to the quantum register. For instance, the qPCA in [9] extracts λ_k from (3) to the quantum register in (2). However, the algorithm in [9] requires a lot of quantum gates and involves approximation in two places.

In this paper we show that

$$|\psi_{A_0}\rangle \xrightarrow{(I \otimes U_{PE})(I \otimes U^+)(CU \otimes I)(I \otimes U_{\lambda, \tau})(I \otimes U_{PE})} |\psi'_A\rangle, \quad (4)$$

which corresponds to a low complexity qPCA algorithm requiring less quantum gates and involving approximation in

only one place. The operations in (4) can be decomposed into following building blocks.

1) Phase estimation $I \otimes U_{PE}$

The purpose of the phase estimation U_{PE} is to extract eigenvalues to the quantum register. Suppose a unitary operator U has an eigenvector $|u\rangle$ with eigenvalue $e^{2\pi i \phi}$, where the ϕ is unknown [8]. Phase estimation [13] can extract the phase ϕ into a quantum register:

$$|0\rangle |u\rangle \xrightarrow{U_{PE}} |\phi\rangle |u\rangle. \quad (5)$$

In our algorithm, the unitary operator $e^{2\pi i A}$ has the eigenvectors u_k with eigenvalues $e^{2\pi i \lambda_k}$, and λ_k can be estimated as

$$|0\rangle |\psi_{A_0}\rangle \xrightarrow{U_{PE}(A)} \sum_{k=1}^r \sigma_k |\lambda_k\rangle |u_k\rangle |v_k\rangle, \quad (6)$$

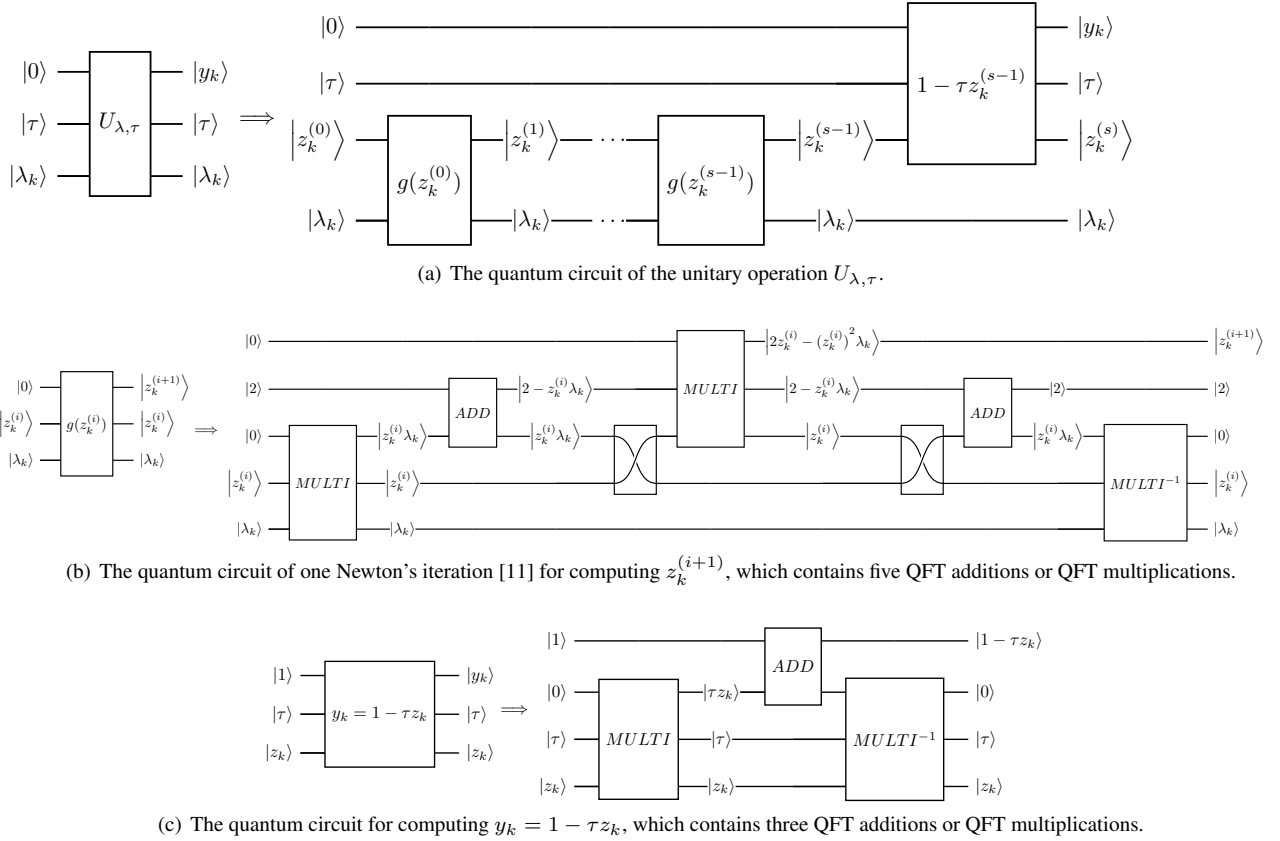


FIGURE 3: The quantum circuit of the Unitary operation $U_{\lambda, \tau}$, which contains eight QFT arithmetic operations [12].

where

$$U_{PE}(A) = (QFT^\dagger \otimes I)(e^{2\pi i A} \otimes I)(H \otimes I). \quad (7)$$

In addition, the register stored $|\psi_{A_0}\rangle$ requires $m = O(\log(pq))$ qubits and the register stored $|\lambda_k\rangle$ requires $n = O(\log(\kappa))$ qubits, where κ is the condition number of the matrix A [14]. The number of the quantum gates required by the U_{PE} operation is $O(n^2)$ [8].

2) Unitary operation $I \otimes U_{\lambda, \tau} \otimes I$

The purpose of the unitary operation $U_{\lambda, \tau}$ is to filter out the small eigenvalues from the quantum register. This is achieved by converting λ_k to $y_k = (1 - \frac{\tau}{\lambda_k})_+ = \max\{1 - \frac{\tau}{\lambda_k}, 0\}$. We first set the intermediate variable $z_k = \frac{1}{\lambda_k}$, which can be obtained numerically by Newton's iteration $z_k^{(i+1)} = 2z_k^{(i)} - (z_k^{(i)})^2 \lambda_k$. This iteration can be implemented by the quantum circuit Fig. 3(b). After obtaining z_k , $y_k = (1 - \tau z_k)_+$ can be obtained by the QFT arithmetic [15], which shown in Fig. 3(c). In summary, the unitary operation $U_{\lambda, \tau}$ for our low complexity qPCA algorithm can be represented as:

$$|0\rangle \sum_{k=1}^r \sigma_k |\lambda_k\rangle |u_k\rangle |v_k\rangle \xrightarrow{U_{\lambda, \tau}} \sum_{k=1}^r \sigma_k |y_k\rangle |\lambda_k\rangle |u_k\rangle |v_k\rangle, \quad (8)$$

and its quantum circuit is given in Fig. 3. In addition, the registers stored $|\tau\rangle$, $|y_k\rangle$ respectively requires the same $n = O(\log(\kappa))$ qubits. The number of the quantum gates required by the $U(\lambda, \tau)$ operation is $O(8 \times (n + n)) = O(16n)$.

3) Unitary controlled operation $CU \otimes I$

The purpose of this step is to employ unitary controlled operation [16] and ancillary qubit to tell whether or not the eigenvalue in the measured quantum bits corresponds to a principal component. If the $y_k > 0$ ($\lambda_k > \tau$), unitary controlled operation will reverse the top qubit (ancillary qubit), otherwise it will do nothing. This procedure can be represented as:

$$\begin{aligned} & |0\rangle \sum_{k=1}^r \sigma_k |y_k\rangle |\lambda_k\rangle |u_k\rangle |v_k\rangle \\ \xrightarrow{CU} & (|1\rangle \sum_{k=1}^t \sigma_k |y_k\rangle |\lambda_k\rangle |u_k\rangle |v_k\rangle \\ & + |0\rangle \sum_{k=t+1}^r \sigma_k |0\rangle |\lambda_k\rangle |u_k\rangle |v_k\rangle). \end{aligned} \quad (9)$$

In addition, the number of the quantum gates required by the CU operation is $O(n)$.

4) Unitary reverse operation $I \otimes U^\dagger$

The purpose of this step is to remove the unnecessary registers that stored the $|y_k\rangle$ and $|\lambda_k\rangle$, we perform the reverse operation of $U_{\lambda,\tau}$ and U_{PE} . The operation procedure can be represented as:

$$\begin{aligned} & (|1\rangle \sum_{k=1}^t \sigma_k |y_k\rangle |\lambda_k\rangle |u_k\rangle |v_k\rangle \\ & + |0\rangle \sum_{k=t+1}^r \sigma_k |0\rangle |\lambda_k\rangle |u_k\rangle |v_k\rangle) \\ \xrightarrow{U^\dagger} & (|1\rangle |0\rangle |0\rangle \sum_{k=1}^t \sigma_k |u_k\rangle |v_k\rangle \\ & + |0\rangle |0\rangle |0\rangle \sum_{k=t+1}^r \sigma_k |u_k\rangle |v_k\rangle). \end{aligned} \quad (10)$$

In addition, the number of the quantum gates required by the U^\dagger operation is $O(16n + n^2)$.

5) Measurement

When we measure the qubits, if the top qubit (ancillary qubit) collapse to 1, it implies that the state of remaining qubits is $|\psi'_{A_0}\rangle = \sum_{k=1}^t \sigma_k |u_k\rangle |v_k\rangle$.

6) The second phase estimation $I \otimes U_{PE}$

To obtain the quantum state $|\psi'_A\rangle = \sum_{k=1}^t \sigma_k |\lambda_k\rangle |u_k\rangle |v_k\rangle$ from $|\psi'_{A_0}\rangle = \sum_{k=1}^t \sigma_k |u_k\rangle |v_k\rangle$, we can perform another phase estimation on $|\psi'_{A_0}\rangle$ shown in Fig. 4, i.e.

$$|\psi'_{A_0}\rangle \xrightarrow{U_{PE}(A)} |\psi'_A\rangle. \quad (11)$$

In addition, the number of the quantum gates required by the second U_{PE} operation is same $O(n^2)$.

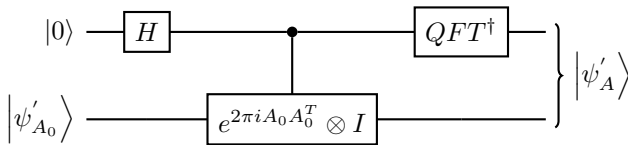


FIGURE 4: The quantum circuit of the second phase estimation, where the input is $|\psi'_{A_0}\rangle$ and the output is $|\psi'_A\rangle$.

The whole procedure of the proposed low complexity qPCA is shown in Algorithm 1 and the corresponding quantum circuit is shown in Fig. 2.

III. COMPLEXITY AND ACCURACY ANALYSIS

In this section, we analyze the circuit complexity and the accuracy of the proposed qPCA algorithm, and compared them with the state-of-the-art qPCA algorithm [9].

Algorithm 1 The low complexity qPCA algorithm.

Input:

A quantum state $|\psi_{A_0}\rangle$;
A unitary operation $U_{PE}(A) = e^{2\pi i A}$;
A threshold constant τ .

Output:

A quantum state $|\psi'_A\rangle$.

Procedure:

- 1: Prepare quantum state $|\psi_1\rangle = |0\rangle |0\rangle |0\rangle |\psi_{A_0}\rangle$.
 - 2: Perform the phase estimation $U_{PE}(A)$ to obtain $|\psi_2\rangle = |0\rangle |0\rangle \sum_1^r \sigma_k |\lambda_k\rangle |u_k\rangle |v_k\rangle$.
 - 3: Perform the unitary operation $U_{\lambda,\tau}$ to obtain $|\psi_3\rangle = |0\rangle \sum_{k=1}^t \sigma_k |y_k\rangle |\lambda_k\rangle |u_k\rangle |v_k\rangle + |0\rangle \sum_{k=t+1}^r \sigma_k |0\rangle |\lambda_k\rangle |u_k\rangle |v_k\rangle$.
 - 4: Perform the controlled operation CU to obtain $|\psi_4\rangle = \sum_{k=1}^t \sigma_k |1\rangle |y_k\rangle |\lambda_k\rangle |u_k\rangle |v_k\rangle + \sum_{k=t+1}^r \sigma_k |0\rangle |0\rangle |\lambda_k\rangle |u_k\rangle |v_k\rangle$.
 - 5: Employ unitary operation U_\dagger to obtain $|\psi_5\rangle = \sum_{k=1}^t \sigma_k |1\rangle |u_k\rangle |v_k\rangle + \sum_{k=t+1}^r \sigma_k |0\rangle |u_k\rangle |v_k\rangle$.
 - 6: Measurement. When the measurement result of the top qubit is 1, the quantum state will collapse to $|\psi'_{A_0}\rangle = \sum_{k=1}^t \sigma_k |u_k\rangle |v_k\rangle$.
 - 7: Extract eigenvalues $|\lambda_k\rangle$ by performing the second phase estimation U_{PE} to get $|\psi'_A\rangle = \sum_{k=1}^t \sigma_k |\lambda_k\rangle |u_k\rangle |v_k\rangle$.
-

A. CIRCUIT COMPLEXITY

First, we analyze the number of qubits required for the quantum circuit of our qPCA. As shown in Fig. 2, register Anc. contains only one ancillary qubit, and the number of the qubits in Reg. A, Reg. B and Reg. C are all $n = O(\log(\kappa))$. Finally, to save $|\psi_{A_0}\rangle$, it requires $O(\log(pq))$ qubits in Reg. M. Therefore the total qubits required for our qPCA is $O(\log(pq\kappa))$, which is the same as the qPCA in [9].

Then we analyze the unitary operations of our qPCA algorithm contained in (4), where each phase estimation U_{PE} requires $O(n^2)$ quantum gates, and the operations $U(\lambda, \tau)$, CU and U^\dagger requires $O(16n)$, $O(n)$, and $O(n^2 + 16n)$ quantum gates, respectively. Therefore, the number of the quantum gates required by our qPCA algorithm is $O(3n^2 + 33n)$. As shown in Fig. 1, it requires much more quantum gates for the qPCA in [9]. The operations $U_{\sigma,\tau}$ and $U'_{\sigma,\tau}$ both require $O(24n)$ quantum gates to compute the Newton's iterations. In addition, the three U_{PE} operations, the two operations $R_y(\alpha)$, and the two operations U^\dagger require $3O(n^2)$, $2O(n)$, and $2O(n^2 + 24n)$ quantum gates, respectively. Therefore the total number of the quantum gates required for the qPCA in [9] is $O(5n^2 + 98n)$.

In summary, the proposed qPCA requires the same number of qubits and much less quantum gates compared with the previous qPCA in [9].

B. THE PRECISION

The approximations of the qPCA in [9] take in two places: parameters estimation and Newton's iterations. However, the approximations of our qPCA only take in Newton's iterations, and even for the Newton's iterations, the proposed qPCA requires less quantum gates since its iterative function has lower order. Therefore, the proposed qPCA has higher level of precision.

IV. EXPERIMENT

In this section, we perform experiments for our low complexity qPCA algorithm on the IBM quantum computing platform: IBM Quantum Experience [17]–[19].

A. THE EXPERIMENT FOR THE 2×2 MATRIX

First, we take the 2×2 matrix

$$A = \begin{bmatrix} 1.5 & 0.5 \\ 0.5 & 1.5 \end{bmatrix} \quad (12)$$

as an example, of which the quantum state is given by [20]

$$|\psi_A\rangle = [0.6708, 0.2236, 0.2236, 0.6708]^T. \quad (13)$$

Notice that the classical PCA should yield

$$\begin{aligned} \lambda_1 &= 2, & u_1 &= [0.7071, 0.7071]^T, \\ \lambda_2 &= 1, & u_2 &= [-0.7071, 0.7071]^T. \end{aligned}$$

When we set the threshold $\tau = 1$, only the eigenvectors u_1 with the eigenvalues λ_1 are reserved, the vector of the algorithm should be given by

$$\frac{\lambda_1 |u_1\rangle |u_1\rangle}{\sqrt{\lambda_1^2}} = [0.5000, 0.5000, 0.5000, 0.5000]^T. \quad (14)$$

The implementation of the quantum circuit for our qPCA algorithm on the IBM Quantum Experience is shown in Fig. 5. Five qubits are required in total. The first qubit q[0] is used as an ancillary qubit. The second to third qubits q[1-2] are used to save eigenvalues $|\lambda_k\rangle$ and $|y_k\rangle$, and the qubits q[3-4] are used to initialize the quantum state $|\psi_A\rangle$. When the measurement result of q[0] is 1, q[3-4] will collapse into the quantum state $|\psi'_A\rangle$.

Circuit Composer on IBM Quantum Experience lets us see how quantum circuits affect the state of a collection of qubits through the measurement probabilities visualizations [21]. As shown in Fig. 7(a), when the top qubit measures 1, the normalized vector of the statistical graph is given by

$$|\psi'_A\rangle_{circuit} = [0.5000, 0.5000, 0.5000, 0.5000]^T. \quad (15)$$

The QASM simulator simulates the execution of quantum circuits and returns counts in histogram, then we run the

quantum circuit on the the QASM simulator, and the result as shown in Fig. 7(b) is given by

$$|\psi'_A\rangle_{qasm} = [0.4859, 0.5245, 0.5143, 0.4735]^T. \quad (16)$$

Similarly, when we set the threshold $\tau = 0.8$, the eigenvectors u_1, u_2 with corresponding the eigenvalues λ_1, λ_2 are reserved, the vector should be given by

$$\frac{\lambda_1 |u_1\rangle |u_1\rangle + \lambda_2 |u_2\rangle |u_2\rangle}{\sqrt{\lambda_1^2 + \lambda_2^2}} \quad (17)$$

$$=[0.6708, 0.2236, 0.2236, 0.6708]^T. \quad (18)$$

and the result of the Circuit Composer is given by

$$|\psi'_A\rangle_{circuit} = [0.6708, 0.2236, 0.2236, 0.6708]^T, \quad (19)$$

the result of QASM simulator is given by

$$|\psi'_A\rangle_{qasm} = [0.6651, 0.2296, 0.2119, 0.6782]^T. \quad (20)$$

B. THE EXPERIMENT FOR THE 4×4 MATRIX

Now we take the 4×4 matrix

$$C = \begin{bmatrix} 0 & 0 & 0 & 0 \\ 0 & 1 & 0 & 0 \\ 0 & 0 & 2 & 0 \\ 0 & 0 & 0 & 3 \end{bmatrix} \quad (21)$$

as another example, of which the corresponding quantum state is given by

$$|\psi_C\rangle = [\dots, 0.2673, \dots, 0.5345, \dots, 0.8018]^T, \quad (22)$$

where the values 0.2673, 0.5345, 0.8018 respectively represent the 6th, 11th, and 16th elements of the vector $|\psi_C\rangle$, and the rest are 0.

Notice that the classical PCA should yield

$$\begin{aligned} \lambda_1 &= 0, & u_1 &= [1, 0, 0, 0]^T, \\ \lambda_2 &= 1, & u_2 &= [0, 1, 0, 0]^T, \\ \lambda_3 &= 2, & u_3 &= [0, 0, 1, 0]^T, \\ \lambda_4 &= 3, & u_4 &= [0, 0, 0, 1]^T. \end{aligned}$$

When we set the threshold $\tau = 1.8$, only the eigenvectors u_3, u_4 with corresponding the eigenvalues λ_3, λ_4 are reserved, the vector should be given by:

$$\begin{aligned} &\frac{\lambda_3 |u_3\rangle |u_3\rangle + \lambda_4 |u_4\rangle |u_4\rangle}{\sqrt{\lambda_3^2 + \lambda_4^2}} \\ &=[\dots, 0.0000, \dots, 0.5547, \dots, 0.8321]^T, \quad (23) \end{aligned}$$

where the values 0.0000, 0.5547, 0.8321 respectively represent the 6th, 11th, and 16th elements of the vector, and the rest are 0.

The implementation of the quantum circuit for our low complexity qPCA algorithm for the matrix C with $\tau = 1.8$ is shown in Fig. 6. The qubits q[0] and q[7] are ancillary qubits and the qubits q[1-2] stored the eigenvalues. The qubits q[3-6] are used to prepare the initial quantum state $|\psi_C\rangle$. When

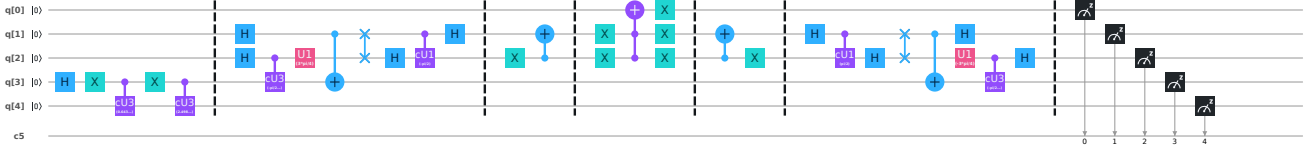


FIGURE 5: The experimental circuit of our qPCA for the 2×2 matrix A with threshold $\tau = 1$ on IBM Quantum Experience. The input of the quantum circuit is $|\psi_A\rangle$, and the output is $|\psi'_A\rangle$. The qubit q[0] is an ancillary qubit. Before the first dash line of the quantum circuit, the qubits q[3-4] are used to initialize the quantum state $|\psi_A\rangle$. Between the first dash and the second dash lines in the quantum circuit, the qubits q[1-2] are used to save eigenvalues from the phase estimation. Between the second and the third dash lines in the quantum circuit, the eigenvalues $|\lambda_k\rangle$ are converted to $|y_k\rangle$ on q[1-2]. Between the third and the fourth dash lines is the controlled operation. The rest of the quantum circuit are the inverse operations and the measurement.

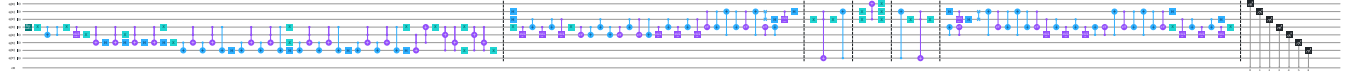
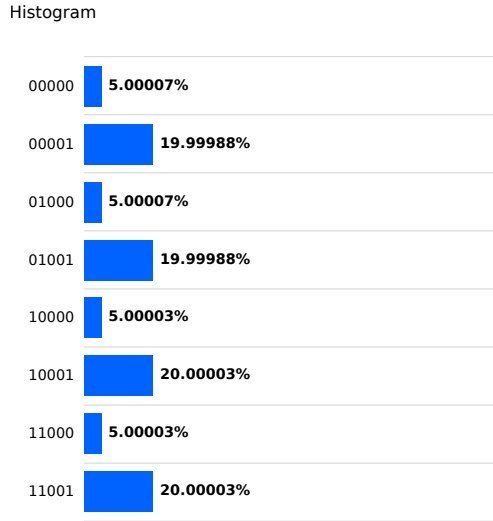
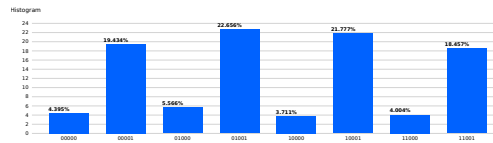


FIGURE 6: The experimental circuit of our qPCA for the 4×4 matrix C with threshold $\tau = 1.8$ on IBM Quantum Experience. The input is the quantum state $|\psi_C\rangle$, and the output is $|\psi'_C\rangle$. The qubits q[0] and q[7] are the ancillary qubits. Before the first dash line of the quantum circuit, the qubits q[3-6] are used to initialize the quantum state $|\psi_C\rangle$. Between the first and the second dash lines in the quantum circuit, the qubits q[1-2] are used to save eigenvalues from the phase estimation. Between the second and the third dash lines in the quantum circuit, the eigenvalues $|\lambda_k\rangle$ is converted to $|y_k\rangle$ on q[1-2]. Between the third and the fourth dash lines is the controlled operation. The rest of the quantum circuit are the inverse operations and the measurement.

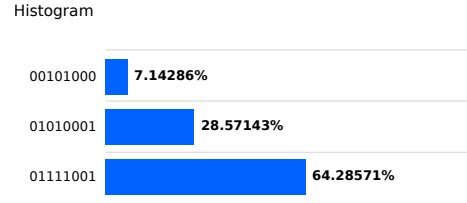


(a) The probability histogram of our qPCA algorithm in the Circuit Composer from IBM Quantum Experience.

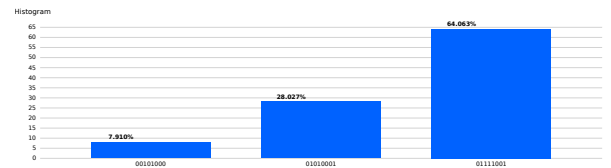


(b) The probability histogram of our qPCA algorithm in the QASM simulator from IBM Quantum Experience.

FIGURE 7: The Circuit Composer (theoretical) result and the QASM simulator result of our qPCA for the 2×2 matrix A with threshold $\tau = 1$ from IBM Quantum Experience.



(a) The probability histogram of our qPCA algorithm in the Circuit Composer from IBM Quantum Experience.



(b) The probability histogram of our qPCA algorithm in the QASM simulator from IBM Quantum Experience.

FIGURE 8: The Circuit Composer (theoretical) result and the QASM simulator result of our qPCA for the 4×4 matrix C with threshold $\tau = 1.8$ from IBM Quantum Experience.

the measurement result of q[0] is 1, q[3-6] will collapse into the quantum state $|\psi'_C\rangle$. The initial quantum state $|\psi_C\rangle$ and the phase estimation operation in the implementation are not straightforward to construct. Therefore we design the binary tree to prepare the initial quantum state, as shown in Fig. 9 of Appendix -A, and the corresponding quantum circuit is shown in Fig. 10. The quantum circuit of the phase estimation on $|\psi_C\rangle$ is shown in Fig. 11 of Appendix -B.

As shown in Fig. 8, the result of the Circuit Composer is given by

$$|\psi'_C\rangle_{circuit} = [\dots, 0.0000, \dots, 0.5547, \dots, 0.8321]^T, \quad (24)$$

and the result of the QASM simulator is given by

$$|\psi'_C\rangle_{qasm} = [\dots, 0.0000, \dots, 0.5294, \dots, 0.8004]^T, \quad (25)$$

where the values 0.0000, 0.5547, 0.8321 respectively represent the 6th, 11th, and 16th elements of the vector $|\psi'_C\rangle_{circuit}$, the values 0.0000, 0.5294, 0.8004 respectively represent the 6th, 11th, and 16th elements of the vector $|\psi'_C\rangle_{qasm}$, and the rest are 0.

Similarly, when we set the threshold $\tau = 0.5$, the eigenvectors u_2, u_3, u_4 with the corresponding eigenvalues $\lambda_2, \lambda_3, \lambda_4$ are reserved, the vector should be given by:

$$\frac{\lambda_2 |u_2\rangle |u_2\rangle + \lambda_3 |u_3\rangle |u_3\rangle + \lambda_4 |u_4\rangle |u_4\rangle}{\sqrt{\lambda_2^2 + \lambda_3^2 + \lambda_4^2}} = [\dots, 0.2673, \dots, 0.5345, \dots, 0.8018]^T, \quad (26)$$

where the values 0.2673, 0.5345, 0.8018 respectively represent the 6th, 11th, and 16th elements of the vector and the rest are 0. The result of the Circuit Composer is given by

$$|\psi'_C\rangle_{circuit} = [\dots, 0.2673, \dots, 0.5345, \dots, 0.8018]^T, \quad (27)$$

and the result of the QASM simulator is given by

$$|\psi'_C\rangle_{qasm} = [\dots, 0.2500, \dots, 0.5484, \dots, 0.7979]^T, \quad (28)$$

where the values 0.2673, 0.5345, 0.8018 respectively represent the 6th, 11th, and 16th elements of the vector $|\psi'_C\rangle_{circuit}$, the values 0.2500, 0.5484, 0.7979 respectively represent the 6th, 11th, and 16th elements of the vector $|\psi'_C\rangle_{qasm}$, and the rest values are 0.

Based on the the experimental results of 2×2 and 4×4 matrices with different threshold respectively, we can see that the Circuit Composer (theoretical) results yielded by our qPCA algorithm are exactly the same as that of classical PCA. For the results yield by quantum computer simulator, our algorithm can also obtain high accuracy. In short, the experimental results meet our expectations.

V. CONCLUSION

In this paper, we propose a low complexity qPCA algorithm, which outputs the quantum state only containing the principal components. This is similar to the state-of-the-art qPCA [9] algorithm. The advantages of the proposed qPCA are as follows: The number of quantum gates required is only about $3/5$ of that of the state-of-the-art; we also show that it has a higher level of precision. Finally we implement the proposed qPCA on IBM Quantum Experience, and the experimental results support our expectations.

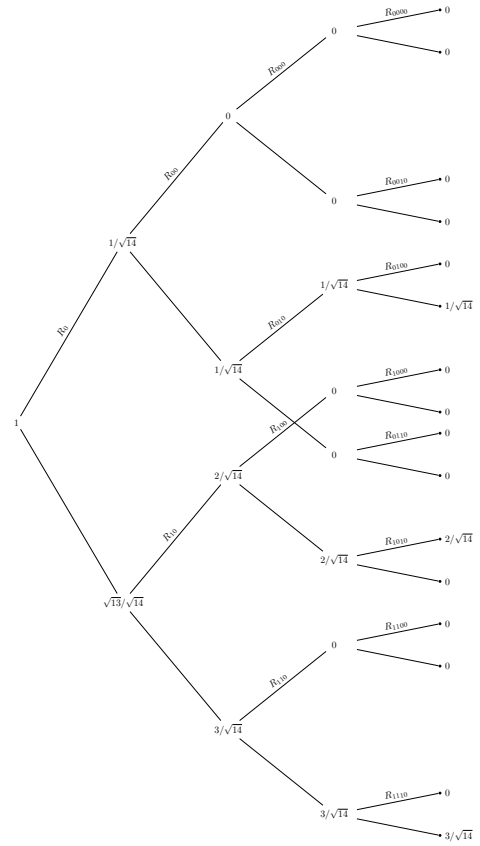


FIGURE 9: The binary tree to prepare the state $|\psi_C\rangle$.

A. THE PREPARATION OF STATE $|\psi_C\rangle$

The initial state $|\psi_C\rangle$ in (22) is not straightforward to prepare on IBM Quantum Experience. Therefore we design the binary tree [22], [23] as shown in Fig. 9 to prepare the quantum state, whose leaf nodes are the vectors of the quantum state, and each branch is a $R_y(\theta)$ unitary operation, where

$$R_y(\theta) = \begin{bmatrix} \cos(\frac{\theta}{2}) & -\sin(\frac{\theta}{2}) \\ \sin(\frac{\theta}{2}) & \cos(\frac{\theta}{2}) \end{bmatrix}. \quad (29)$$

The corresponding quantum circuit of the binary tree is shown in Fig. 10.

B. THE PHASE ESTIMATION OF MATRIX C

The quantum circuit of the phase estimation on the matrix C is not straightforward to design on IBM Quantum Experience. Therefore we decompose the phase estimation into several unitary operations which can be implemented by simple quantum gates [24], [25]. The unitary matrices in the phase estimation of C are $U_1 = e^{\frac{2\pi i C}{4}}$, $U_2 = e^{\frac{2\pi i C}{2}}$ [26], [27], where

$$U_1 = \begin{bmatrix} 0 & 0 & 0 & 0 \\ 0 & i & 0 & 0 \\ 0 & 0 & -1 & 0 \\ 0 & 0 & 0 & -i \end{bmatrix}, \quad U_2 = \begin{bmatrix} 0 & 0 & 0 & 0 \\ 0 & -1 & 0 & 0 \\ 0 & 0 & 1 & 0 \\ 0 & 0 & 0 & -1 \end{bmatrix}. \quad (30)$$

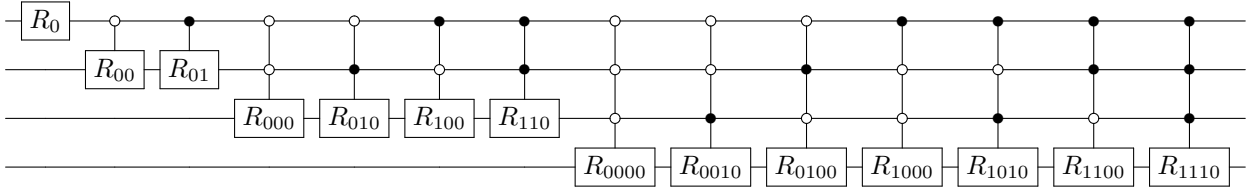
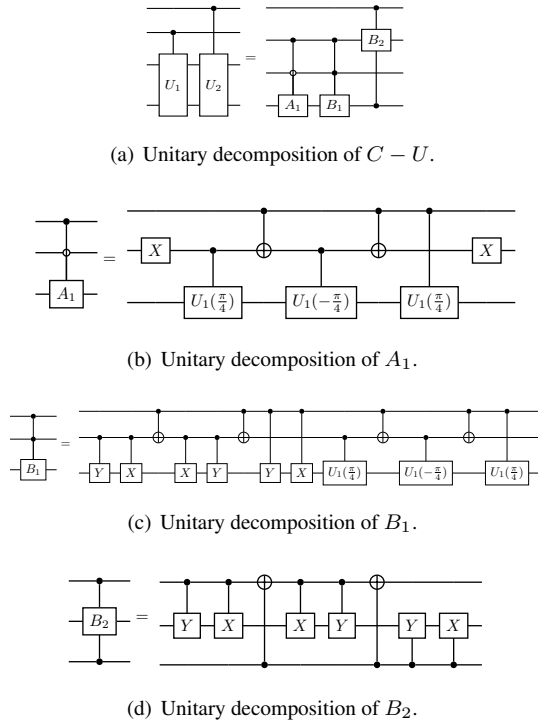


FIGURE 10: The quantum circuit to prepare the state $|\psi_C\rangle$.



(a) Unitary decomposition of $C - U$.

(b) Unitary decomposition of A_1 .

(c) Unitary decomposition of B_1 .

(d) Unitary decomposition of B_2 .

FIGURE 11: The unitary operation of the phase estimation of the matrix C .

The corresponding quantum circuits of $C - U_1$, $C - U_2$ are show in Fig. 11.

REFERENCES

- [1] M. E. Wall, A. Rechtsteiner, and L. M. Rocha, "Singular value decomposition and principal component analysis," in *A practical approach to microarray data analysis*. Springer, 2003, pp. 91–109.
- [2] S. Karamizadeh, S. M. Abdullah, A. A. Manaf, M. Zamani, and A. Hooman, "An overview of principal component analysis," *Journal of Signal and Information Processing*, vol. 4, no. 3B, p. 173, 2013.
- [3] J. Shlens, "A tutorial on principal component analysis," arXiv preprint arXiv:1404.1100, 2014.
- [4] R. Bro and A. K. Smilde, "Principal component analysis," *Analytical Methods*, vol. 6, no. 9, pp. 2812–2831, 2014.
- [5] S. Lloyd, M. Mohseni, and P. Rebentrost, "Quantum principal component analysis," *Nature Physics*, vol. 10, pp. 631–633, 2014.
- [6] C. Shao, "An improved algorithm for quantum principal component analysis," arXiv preprint arXiv:1903.03999, 2019.
- [7] M. A. Nielsen and I. Chuang, "Quantum computation and quantum information," 2002.
- [7] C.-H. Yu, F. Gao, S. Lin, and J. Wang, "Quantum data compression by principal component analysis," *Quantum Information Processing*, vol. 18, no. 8, p. 249, 2019.
- [9] J. Lin, W.-S. Bao, S. Zhang, T. Li, and X. Wang, "An improved quantum principal component analysis algorithm based on the quantum singular threshold method," *Physics Letters A*, vol. 383, no. 24, pp. 2862–2868, 2019.
- [10] B. Duan, J. Yuan, Y. Liu, and D. Li, "Efficient quantum circuit for singular-value thresholding," *Physical Review A*, vol. 98, no. 1, p. 012308, 2018.
- [11] M. K. Bhaskar, S. Hadfield, A. Papageorgiou, and I. Petras, "Quantum algorithms and circuits for scientific computing," arXiv preprint arXiv:1511.08253, 2015.
- [12] E. Şahin, "Quantum arithmetic operations based on quantum fourier transform on signed integers," arXiv preprint arXiv:2005.00443, 2020.
- [13] W. van Dam, G. M. D'Ariano, A. Ekert, C. Macchiavello, and M. Mosca, "Optimal quantum circuits for general phase estimation," *Physical review letters*, vol. 98, no. 9, p. 090501, 2007.
- [14] I. Goodfellow, Y. Bengio, and A. Courville, *Deep Learning*. MIT Press, 2016, <http://www.deeplearningbook.org>.
- [15] L. Ruiz-Perez and J. C. Garcia-Escartin, "Quantum arithmetic with the quantum fourier transform," *Quantum Information Processing*, vol. 16, no. 6, p. 152, 2017.
- [16] D. P. DiVincenzo, "Quantum gates and circuits," *Proceedings of the Royal Society of London. Series A: Mathematical, Physical and Engineering Sciences*, vol. 454, no. 1969, pp. 261–276, 1998.
- [17] A. Cross, "The ibm q experience and qiskit open-source quantum computing software," *APS*, vol. 2018, pp. L58–003, 2018.
- [18] P. Balasubramanian, B. Behera, and P. Panigrahi, "Circuit implementation for rational quantum secure communication using ibm q experience beta platform."
- [19] D. García-Martín and G. Sierra, "Five experimental tests on the 5-qubit ibm quantum computer," arXiv preprint arXiv:1712.05642, 2017.
- [20] P. J. Coles, S. Eidenbenz, S. Pakin, A. Adedoyin, J. Ambrosiano, P. M. Anisimov, W. Casper, G. Chennupati, C. Coffrin, H. Djidjev et al., "Quantum algorithm implementations for beginners," arXiv: Emerging Technologies, 2018.
- [21] IBM, "Ibm quantum experience," <https://quantum-computing.ibm.com/>.
- [22] L. Grover and T. Rudolph, "Creating superpositions that correspond to efficiently integrable probability distributions," arXiv preprint quant-ph/0208112, 2002.
- [23] I. Kerenidis and A. Prakash, "Quantum recommendation systems," arXiv preprint arXiv:1603.08675, 2016.
- [24] J. J. Vartiainen, M. Möttönen, and M. M. Salomaa, "Efficient decomposition of quantum gates," *Physical review letters*, vol. 92, no. 17, p. 177902, 2004.
- [25] C.-K. Li, R. Roberts, and X. Yin, "Decomposition of unitary matrices and quantum gates," *International Journal of Quantum Information*, vol. 11, no. 01, p. 1350015, 2013.
- [26] H. Mohammadbagherpoor, Y.-H. Oh, A. Singh, X. Yu, and A. J. Rindos, "Experimental challenges of implementing quantum phase estimation algorithms on ibm quantum computer," arXiv preprint arXiv:1903.07605, 2019.
- [27] S. Dutta, A. Suau, S. Dutta, S. Roy, B. K. Behera, and P. K. Panigrahi, "Demonstration of a quantum circuit design methodology for multiple regression," arXiv preprint arXiv:1811.01726, 2018.

...